Inorganic Chemistry

Article

pubs.acs.org/IC

Probing the Chemical Nature of Dihydrogen Complexation to Transition Metals, a Gas Phase Case Study: H_2−CuF

Daniel J. Frohman,[†] G. S. Grubbs, II,*[,†] Zhenhong Yu,[‡] and Stewart E. Novick[†]

[†]Department of Chemistry, Wesleyan University, 52 Lawn Avenue, Middletown, Connecticut 06459-0180, United States

[‡]Aerodyne Research, Inc., 45 Manning Road, Billerica, Massachusetts 01821-3976, United States

Supporting Information

ABSTRACT: This work details a gas phase study of the bonding of hydrogen to the metal in a simple diatomic analogue of a metal organic framework (MOF), copper fluoride, via dihydrogen complexation. This is the first microwave study of these types of interactions. $J = 1-0$ transitions of *para*-H_2−CuF, *ortho*-D_2−CuF, and HD−CuF have been measured and analyzed. The complexes were prepared by laser ablating a metal copper rod in the presence of a gas mix of 0.6% SF_6 and 3% H_2 in Ar undergoing supersonic expansion. The binding energy of this complex is addressed through quantum chemical calculations and measured nuclear quadrupole coupling constants for copper and deuterium. The significant change in the calculated binding energy and nuclear quadrupole coupling constants in relation to similar molecules suggest bonding greater than that typical of van der Waals interactions.

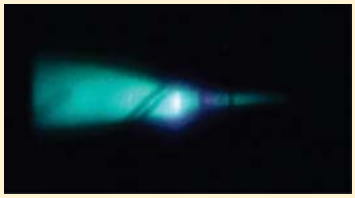

INTRODUCTION

Hydrogen has long been investigated as a clean, abundant energy carrier. Hydrogen is an excellent energy carrier by mass, providing for almost three times the combustion energy of gasoline per unit mass. Currently it is estimated that one-third of the energy consumption of industrialized nations is used in transportation.[1] A major scientific challenge for hydrogen application in transportation is the development of a safe and inexpensive hydrogen storage method. One possible solution would be the adsorption of hydrogen to a solid surface or in bulk material allowing for smaller, more compact storage of hydrogen for convenient use.[2−5]

A breakthrough in hydrogen storage comes from the introduction of metal−organic frameworks (MOFs), which are coordination crystalline polymers formed by connecting transition metal ions with organic linkers.[6−9] Molecular storage within the open cages of the MOF offers an opportunity to correlate chemical structure with specific functionality such as hydrogen adsorption.[10] The understanding of hydrogen coordination with the metal center is therefore critical for the future development of MOFs for hydrogen storage applications and is the motivation behind this study. Coordination complexes of molecular hydrogen with transition metals known as dihydrogen complexes have been extensively studied since their discovery by Kubas and co-workers in 1984,[11−15] and their theory is well understood.[16−20] Currently, structural information of dihydrogen complexes is provided predominantly by neutron diffraction, inelastic neutron scattering, IR, and NMR spectroscopies.[11,21−26] The requirement for a large single crystal hinders neutron diffraction's application to most of the known complexes. Inelastic neutron scattering provides insight into the internal rotation of the bound hydrogen but is limited in its ability to only study this motion given its resolution.[26] IR data on the complex is a good characterization and geometric structural tool but does not give much insight into the electronic structure of the system in question. On the other hand, the dipolar coupling measured by the NMR technique is proportional to $(d_{HH})^{-3}$ and breaks down at longer H−H distances.

This work presents the Fourier transform microwave (FTMW) spectrum of the dihydrogen complex *para*-H_2−CuF. CuF represents a very basic model of an active site in MOFs for hydrogen storage by utilizing a common metal involved in MOFs.[27,28] FTMW spectroscopy, in turn, is a superb technique to investigate molecular structure and electronic properties in the gas phase[29,30] by measuring rotational transitions of the studied molecules. As a background-free technique in principle, FTMW spectroscopy only requires the sample to have a permanent dipole moment and sufficient concentration ($\approx 10^{-9}$ mol per gas pulse) to detect species for study. In the past few decades, FTMW spectroscopy has served as an important tool for testing the feasibility of theoretical methods of electronic structure calculations and offered valuable information on both molecular structure and energy.[31−34] The richness of the rotational spectrum of isotopic hydrogen-transition metal complexes provides us the opportunity to study, in detail, the structure and bonding involved in the adsorption of hydrogen in MOFs. In this work the authors report, to their knowledge, the first FTMW observation of a dihydrogen complex to a metal containing molecule, CuF.

EXPERIMENTAL SECTION

Apparatus and Synthesis. All experiments were performed with a Balle-Flygare type[35] cavity, pulsed jet FTMW spectrometer with laser ablation source functioning in the 6−26.5 GHz frequency range. The

Received: September 5, 2012
Published: January 9, 2013

   dx.doi.org/10.1021/ic301941k | *Inorg. Chem.* 2013, 52, 816−822

details of this experiment have been described in earlier work.[36,37] This experiment utilizes a Fabry-Pérot resonator consisting of curved aluminum mirrors separated by approximately 76 cm. The resonator is frequency tuned by moving one of the mirrors while the other remains stationary. The spectrometer is held at a pressure of 10^{-9} bar, and samples of gas are introduced to the spectrometer through a 0.8 mm diameter pulsed nozzle mounted on the back of the stationary mirror. This parallel orientation of the gas jet and cavity axis increases sensitivity and resolution of the spectrometer while also producing spectra which are Doppler doubled. After the firing of the gas nozzle, microwaves are pulsed into the chamber and the electric dipoles of the molecules begin to align and orient themselves with the microwave's electric field vector. After the microwaves are turned off, the molecules begin to relax and the resulting free induction decay (FID) is collected in the time domain. The transition signal is amplified and Fourier transformed into the frequency domain for analysis. Uncertainty in the line centers are 1 kHz. Sample spectra are presented in Figures 1 and 2. Given the current spectrometer setup, only neutral species, not ions, are observed.

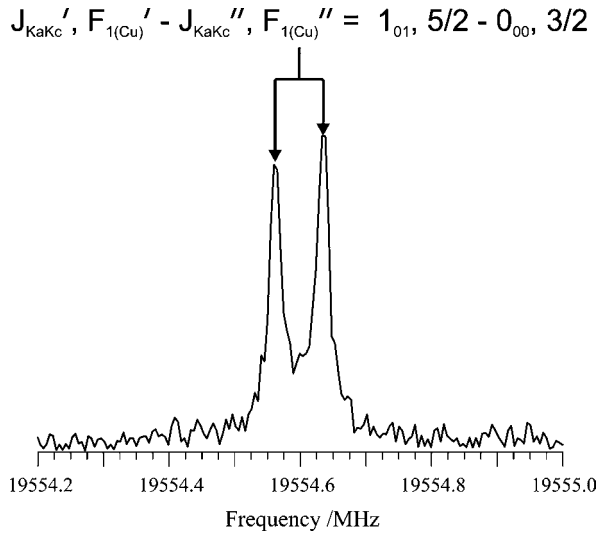

Figure 1. Observed J_{KaKc}', $F_{1(Cu)}'$–J_{KaKc}'',$F_{1(Cu)}''$ = 1_{01}, 5/2 − 0_{00}, 3/2 transition of *para*-H_2–CuF. The transition was recorded at 19554.5985 MHz using a FID of 1K data points for 1500 nozzle pulses. Signal-to-noise is 24:1. 2K data points were used for fluorine hyperfine structure.

A laser ablation source of the Walker–Gerry design[38] is attached to the end of the nozzle. The laser ablation source utilizes the fundamental (1064 nm) of a Polaris II Nd:YAG laser focused onto a translating and traversing copper metal rod. When the gas is pulsed, a gas mix consisting of 0.6% SF_6 and 3% H_2 in Ar enters the laser ablation jig undergoing a supersonic expansion. Downstream from the point of entry of the gas is the spinning rod slightly recessed from the channel in which the gas propagates. Toward the end of the gas pulse, the laser is fired and focused onto the metal rod creating a plasma. The plasma is entrained in the supersonic expansion, and reactions occur which create new molecules and complexes within the expanding jet as it enters the spectrometer. For a more technical overview, the ablation jig has been described in greater detail elsewhere.[37]

Gas sample composition, carrier gases, and timings were chosen based upon previous successes of laser ablated species[37] and personal successes in obtaining the best signal-to-noise spectra reported for the previously studied *p*-H_2–OCS complexes.[39−41] Backing pressures of 4.5−5 bar were used in accordance with that of the rare gas complex, Ar–CuF.[42] Although *p*-H_2–OCS complexes needed a He carrier to be observed because of competition of the more strongly binding noble gases,[39−41] that is not an issue here, and Ar, which produces colder rotational temperatures (1−4K),[43,44] was chosen as the carrier gas. Lower rotational temperatures increase the population of the very low

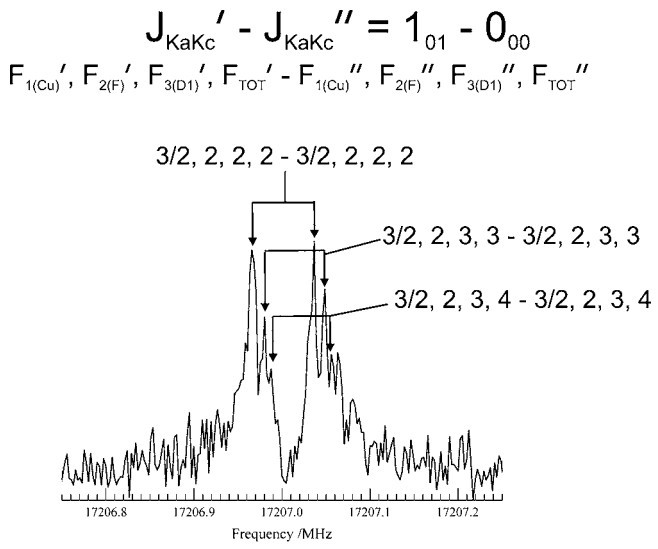

Figure 2. Part of the observed 1_{01}–0_{00} transition of *ortho*-D_2–CuF. The transition is split by the hyperfine nuclear quadrupole interaction of the two deuterium nuclei. The labeled transitions are the 3/2,2,2,2–3/2,2,2,2 transition measured at 17207.0013 MHz; the 3/2,2,3,3–3/2,2,3,3 transition measured at 17207.0143 MHz; and the 3/2,2,3,4–3/2,2,3,4 transition measured at 17207.0220 MHz. These four quantum numbers are F_1, F_2, F_3, and F_{TOT}, as described in the text. The nuclear spins of the Cu, F, $D_{(1)}$, and $D_{(2)}$ are coupled, in order. The transitions are all Doppler-doubled. This spectrum is the result of adding the free induction decay of 2500 gas pulses.

J states which, in turn, give larger signal-to-noise ratios of transitions involving these states. Excited vibrational states of the complex were not looked for, but similar experiments on metal halide diatomics put the vibrational temperatures < 400 K.[44,45] In this experiment, the gas was pulsed for approximately 500 μs. The laser was fired approximately 10 μs before the end of the gas pulse allowing for the gas mix to travel toward the rod and pick up the plasma and react. The plume resulting from the laser ablation consists of ground state and excited state metal atoms and ions. The characteristic color of the plume results from the emission of the excited atoms and ions; this is teal in the case of copper. A picture of the copper plume is shown in Figure 3. The magnitude of the visual plume is used to optimize laser alignment on the copper rod target.

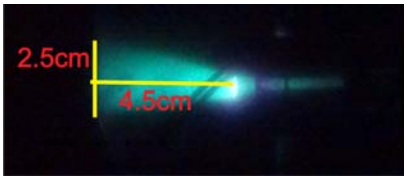

Figure 3. Plume created from the laser ablation of the copper. The plume is 4.5 cm by 2.5 cm.

■ QUANTUM CHEMICAL CALCULATIONS

All calculations were performed on the Gaussian Developmental Version Program Suite.[46] The calculations were performed utilizing the density functional APF-D method[47] along with an aug-cc-pVQZ[48] basis sets for H and F with an effective core potential, ECP10MDF_AVQZ,[49,50] from the Stuttgart Web site[51] for Cu. A special feature of an APF-D method is that the counterpoise correction is not necessarily needed in calculating molecular interactions and, therefore, counterpoise was not used in this work.[47] Equilibrium and

dx.doi.org/10.1021/ic301941k | Inorg. Chem. 2013, 52, 816−822

vibrationally averaged (r_0) structures have been determined. The calculated equilibrium structure is presented in Figure 4.

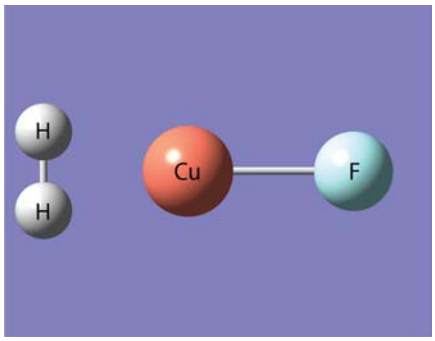

Figure 4. APF-D calculated r_e structure of the H_2−CuF dihydrogen complex. The calculation was performed with an ECP10MDF effective core potential for the copper core electrons along with an aug-cc-pVQZ basis for the remaining electrons. The calculated structure is predicted to have an equilibrium dissociation energy of 105 kJ mol^{-1} with a Cu to center-of-mass (C.O.M) of H_2 distance of 1.51 Å. The equilibrium Cu−F bond distance in the complex is predicted to be 1.738 Å, and the H−H equilibrium bond distance is predicted to be elongated to 0.8120 Å.

The picture was rendered using GaussView 5.0.[52] The calculated r_0 structure is presented as part of Table 5. The calculated dissociation energy, D_e, for H_2−CuF → H_2 + CuF, is 105 kJ mol^{-1} (8800 cm^{-1} or 25 kcal mol^{-1}), a bond strength between that of a weakly bound complex and a strong covalent bond. The calculated equilibrium and vibrationally averaged structure is T-shaped and of C_{2v} symmetry.

Mulliken and atomic polar tensor (APT) charges from the APF-D calculation were used to aid in the determination of the oxidation state of the copper atom. Mulliken charges for each atom are +0.15, −0.61, +0.23, and +0.23 while APT values are +0.45, −0.66, +0.10, and +0.10 for Cu, F, H, and H, respectively. These calculations support an oxidation state of +1 for the copper. For this calculation to be consistent with an oxidation state Cu(III) for H_2−CuF (that is, for the molecule to be the hydride, $Cu(H)_2F$), the charge on copper would be greater than one and the charges on the hydrogens would be negative.

Along with calculated structures and charges, molecular orbitals were determined for H_2, CuF, and H_2−CuF. Pictures of these orbitals are given in Figure 5. The orbitals were rendered in GaussView 5.0 as well.[52] This was useful in the analysis of the chemical nature of the interaction and will be explained in detail in the Results and Discussion section.

RESULTS AND DISCUSSION

Spectra of H_2−CuF. The calculations outlined earlier were used as the basis for search regions for the spectrometer. The rotational constants A_e, B_e, and C_e were calculated to be 1492424.0 MHz, 9850.8 MHz, and 9786.2 MHz, respectively, while the ground vibrational constants A_0, B_0, and C_0 were calculated to be 1484546.8 MHz, 9795.1 MHz, and 9718.7 MHz, respectively. Because the A constant was very high in frequency (outside the range of our spectrometer) and the dipole of the molecule lying along the a-axis, only the a-type transitions involving B and C were investigated. For J = 1−0 transitions there is only one transition of this type, $J = 1_{01}-0_{00}$,

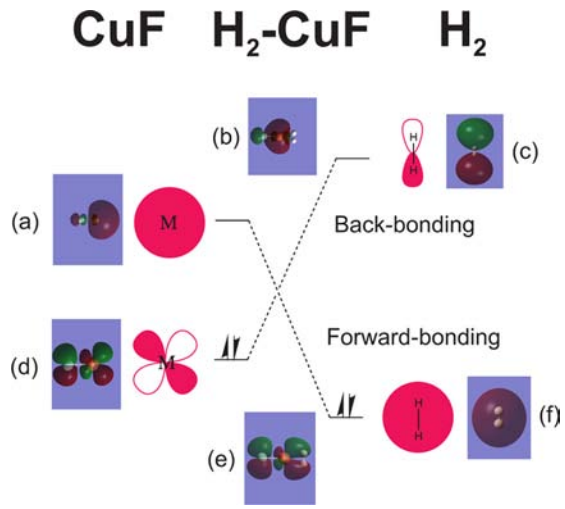

Figure 5. Schematic of the σ transition metal complexation[16−19] of H_2 to CuF. The center shows the interactions while the pictures are renderings of the calculated molecular orbitals for the individual monomers and the complex. Only the most important orbitals and interactions involved in the bonding are shown. The HOMO of H_2, f, interacts with the LUMO of the CuF, a, forming the forward-bonding interaction, orbital b. The shape of orbital b is influenced by the HOMO of CuF which is not shown. The LUMO of H_2, c, is capable of overlap with lower level π-type orbitals, d, from CuF providing the backbonding (shown in e) and should result in the elongation of the H_2 bond.

whose frequency is $B + C$, which is predicted to be at 19514 MHz ignoring hyperfine splitting.

Within the search, three transitions of significant signal strength corresponding to the three J = 1−0 nuclear electric quadrupole coupling transitions of ^{63}Cu (I = 3/2) were observed between 19540 and 19570 MHz, less than 1% from the predicted value mentioned above. One of these transitions is shown in Figure 1. These transitions were tested for laser (Cu), SF_6, and H_2 dependency by individually eliminating them from the experiment and observing the transition's disappearance.

After observation of p-H_2−CuF, searches for isotopic substitutions at each hydrogen atom and at the copper were undertaken utilizing gas mixes involving D_2 and HD and observing the spectra of the ^{65}Cu in natural abundance. Search regions were determined by using the original calculated structure for p-H_2−CuF and substituting the appropriate atom with the new isotope. The ratio of the measured rotational constants to the calculated constants of p-H_2−CuF was multiplied by the calculated rotational constants of o-D_2−CuF and HD−CuF in order to obtain "scaled" predictions for the transition frequencies of these isotopologues. Frequencies of all the isotopically substituted transitions reported are within 4 MHz of their predicted values.

Fluorine hyperfine structure was observed and reported in the previous study of Ar−CuF,[42] leading us to also test for this. At 1K data points (9.76 kHz between points in the spectra obtained by the Fourier transformation of a ≈100 μs free induction decay), however, this was not observed in H_2−CuF. Moving to 2K data points resulted in higher resolution of the peaks and the ability to define these splittings. Moving to higher resolution did not resolve out all of the transitions and, in these cases, the 1K measured frequency was assigned as the predicted strongest hyperfine component.

dx.doi.org/10.1021/ic301941k | Inorg. Chem. 2013, 52, 816−822

Table 1. Spectroscopic Parameters for *para*-H_2−CuF, *ortho*-D_2−CuF, and HD−CuF

	^{63}Cu			^{65}Cu		
parameter	*para*-H_2−CuF	HD−CuF	*ortho*-D_2−CuF	*para*-H_2−CuF	HD−CuF	*ortho*-D_2−CuF
$(B + C)/2$ MHz	9778.807(1)[a]	9141.6421(1)	8597.3468(6)	9732.190(1)	9105.850639(7)	8569.6822(3)
eQq_{Cu} MHz	61.275(2)	61.461(1)	61.713(7)	56.673(7)	56.86760(7)	57.089(4)
$C_{I_{Cu}}$ kHz	28.(1)	27.7(1)	21.7(8)	31.(1)	31.448(9)	25.6(4)
C_{I_F} kHz	−8.(4)	−7.0(6)	−9.(4)	−8.(4)	−7.81(4)	−8.(2)
α_{Cu-F}[b] kHz	[−1.53]	[−1.53]	[−1.53]	[−1.71]	[−1.71]	[−1.71]
eQq_{D1} kHz		41.(3)	47.(7)		47.20(7)	50.(4)
eQq_{D2} kHz			47.(7)			50.(4)
N[c]	5	9	8	5	14	9
RMS[d] kHz	2.0	0.7	2.2	2.0	2.4	1.4

[a]Numbers in parentheses give standard errors (1σ, 67% confidence level) in units of the least significant figure. [b]Value held to the literature value reported in Ar−CuF.[42] [c]Number of observed transitions used in the fit. [d]Root mean square deviation of the fit, $(\sum[(\text{obs} - \text{calc})^2]/N \text{ lines})^{1/2}$.

Assignment. Measured frequencies with their quantum number assignment are given in the Supporting Information. Frequencies were assigned and the spectroscopic parameters were fit using Pickett's SPFIT and SPCAT software.[53] Although H_2−CuF is of C_{2v} symmetry and thus an asymmetric top, the molecule was fit to a Hamiltonian for a linear molecule because the only observable transition, 1_{01}−0_{00}, requires the determinable rotational constant combination to be $(B + C)/2$ (as a replacement for the B_0 term in a linear Hamiltonian). It has already been mentioned that there is ^{63,65}Cu ($I = 3/2$) and ^{19}F ($I = 1/2$) hyperfine splitting of the rotational transition. Further hyperfine splitting is caused by the quadrupolar nucleus of deuterium ($I = 1$) in HD and D_2. All isotopologues were fit.

Angular momentum coupling schemes for these molecules follow $\mathbf{J} + \mathbf{I}_{Cu} = \mathbf{F}_1$, $\mathbf{F}_1 + \mathbf{I}_F = \mathbf{F}_{TOT}$ for *p*-H_2−^{63}CuF and *p*-H_2−^{65}Cu. For HD−^{63}CuF and HD−^{65}CuF, the coupling scheme is $\mathbf{J} + \mathbf{I}_{Cu} = \mathbf{F}_1$, $\mathbf{F}_1 + \mathbf{I}_F = \mathbf{F}_2$, and $\mathbf{F}_2 + \mathbf{I}_D = \mathbf{F}_{TOT}$. Lastly, for *o*-$D_2$−^{63}CuF and *o*-$D_2$−^{65}CuF, the coupling scheme for fitting is $\mathbf{J} + \mathbf{I}_{Cu} = \mathbf{F}_1$, $\mathbf{F}_1 + \mathbf{I}_F = \mathbf{F}_2$, $\mathbf{F}_2 + \mathbf{I}_{D1} = \mathbf{F}_3$, and $\mathbf{F}_3 + \mathbf{I}_{D2} = \mathbf{F}_{TOT}$, where **J** is the angular momentum for rotation of the molecule, **I** refers to the various nuclear spins of the atoms, and the **F**'s are the intermediate angular momenta. *p*-H_2−CuF is, of course, the nuclear spin 0 state of H_2, which is of odd parity with respect to interchange of the identical nuclei, while *o*-D_2−CuF corresponds to nuclear spin states of 0 and 2 and is of even parity.

We will show that H_2−CuF is T-shaped. Thus, rotation about the *a* axis interchanges the two identical hydrogen nuclei, which are fermions. The total wave function must be antisymmetric with respect to the interchange of the two hydrogens (negative parity) and $\Psi_{tot} = \Psi_{spin} \times \Psi_{rot} \times \Psi_{vib} \times \Psi_{elec}$. Ψ_{vib} and Ψ_{elec} are of positive parity; $\Psi_{rot} \sim (-1)^K$ and $K = 0$; therefore, Ψ_{rot} is of positive parity. Therefore Ψ_{spin} must be of negative parity, that is, the *para* state, $(1/\sqrt{2})(\alpha\beta - \beta\alpha)$, of H_2. D_2, by contrast, is composed of two bosons, and for D_2-CuF, the total wave function must therefore be of positive parity with respect to the interchange of the two deuterium nuclei. Thus for D_2-CuF, Ψ_{spin} must be of positive parity, which is the *ortho* state, $I_{tot,D} = 0$ and 2.

The fitted parameters are presented in Table 1. As shown in the table, the rotational constant, $(B + C)/2$, Cu and D nuclear quadrupole coupling constants (eQq), nuclear spin-rotation parameters (C_I) for Cu and F, and the nuclear spin−spin (α_{Cu-F}) term for Cu−F were needed for a satisfactory fit. Typically a fit of this nature would also consist of the centrifugal distortion constant, D_J, but at least two different sets of transitions in J are needed to appropriately fit this term causing the reported $(B + C)/2$ to be slightly enlarged. Also due to the small data set, α_{Cu-F} was fixed to that reported in Ar−CuF[42] but needed for a satisfactory fit to experimental uncertainty.

Structure and Bonding. The first notable difference in this spectra, as compared to the previous CuF monomer work,[42,54] is the large separation in the quadrupole transitions leading to the augmented value of the eQq due to copper; 61.275(2) MHz for H_2−CuF versus 21.95(10) MHz[54] for the monomer. The nuclear quadrupole coupling constant is a direct measure of the electric field gradient at the nucleus with the nuclear spin and, therefore, gives insight into the bonding nature of the atom involved.[55−57] ArCuF (eQq of ^{63}Cu, 38.0556(15) MHz),[42] KrCuF (41.77(3) MHz),[58] XeCuF (47.76(11) MHz),[59] N_2−CuF (61.8825(8) MHz),[60] and OC−CuF (75.406(19) MHz)[61] all had similar enlargements of their eQq(Cu) value upon complexation. Typical van der Waals interactions, though, have little to no effect on the value of the coupling constant (either χ_{zz} or eQq) in the axis system of the uncomplexed monomer.[62,63] Thus it was argued that the augmentation of the eQq(Cu) values of ArCuF, KrCuF, XeCuF, and OC−CuF along with the supporting binding energy calculations for the complexes (47, 45, and 63, and 150 kJ mol^{-1},[64] respectively) show the beginning of chemical bonding between the rare gas or CO and the copper fluoride.[42,58,59,61] Table 2 compares the rare gas complexes along with the measured N_2−CuF and OC−CuF complexes to that of H_2−CuF. The eQq(Cu) (61.275(2) MHz) and calculated binding energy (105 kJ mol^{-1}) of H_2−CuF is larger than all rare gas complexes of CuF[42,58,59] but is less than that of the N_2−CuF and OC−CuF complexes,[60,61] suggesting the beginning of chemical bonding between H_2 and CuF.

Chemical interactions of the H_2 molecule with a metal center have precedence in inorganic chemistry and are known as σ complexes, most notably, dihydrogen complexes, for which there are numerous examples.[11−15,21−25] A typical σ complex is analogous to traditional π backbonding.[16] In these complexes, electrons in a σ bonding orbital of H_2 donate into an empty d_σ type orbital on the metal forming the bond. In addition, the metal donates electron density from a d_π orbital to the antibonding σ^* orbital of H_2, elongating the H−H bond distance.[16−19] H_2−CuF is an analogous case, but instead of an empty d_σ orbital the interaction is with the LUMO of CuF on copper which has a substantial amount of *s* character. In this case, the σ orbital of H_2 overlaps with this partially *s*-type orbital on the copper. In addition, there is electron donation from the

dx.doi.org/10.1021/ic301941k | Inorg. Chem. 2013, 52, 816−822

metal d_π orbital into the H_2 σ^* orbital. These interactions are presented with the orbital pictures in Figure 5.

The shifts in electron donation in asymmetric orbitals can be observed spectroscopically through measurement of the nuclear electric quadrupole coupling constant, eQq.[55−57,65] As shown in Tables 2 and 3, there is a significant change in the eQq values of copper and deuterium upon complexation, and this is directly related to the binding energy of the complex. There is a linear relationship between the calculated binding energy and the measured eQq of the complex given in Table 2 as shown by the plot in Figure 6. The predicted equilibrium binding energy for p-H_2−CuF is 105 kJ mol^{-1} by the method given in the Quantum Chemical Calculations section above. This value is significantly larger than typical van der Waals interactions and hydrogen bonding (<5 kJ mol^{-1} and ∼15 kJ mol^{-1}, respectively),[66] suggesting chemical bonding is taking place. Table 3 compares the known van der Waals interaction HD− and D_2−OCS with known, individually bonded, terminal dihydride systems (in this case, deuterium) involving rhenium, Re. The deuterium eQq values in Table 3 show qualitatively and quantitatively that the dihydrogen complex p-H_2−CuF lies somewhere between the values in the van der Waals bonded OCS and the covalent D_2 rhenium complexes giving credence to the beginnings of a chemical bond in H_2−CuF.

Table 2. Comparison of ^{63}Cu Nuclear Quadrupole Coupling Constants among X−CuF Complexes and Related Species along with Their Reported/Calculated Dissociation Energies

species	^{63}Cu eQq values (MHz)	D_e (kJ mol^{-1}) of complex
CuF	21.95(10),[a,54] 21.9562(24)[42]	
^{40}Ar−CuF	38.0556(15)[42]	47[42]
^{84}Kr−CuF	41.77(3)[58]	45[58]
^{132}Xe−CuF	47.76(11)[59]	63[59]
p-H_2−CuF	61.275(2)[b]	105[b]
N_2−CuF	61.8825(8)[60]	139[60]
OC−CuF	75.406(19)[61]	150[64]

[a]Numbers in parentheses give standard errors (1σ, 67% confidence level) in units of the least significant figure. [b]This work.

Table 3. Comparison of Deuterium Nuclear Quadrupole Coupling Constants among HD and D_2 Related Species

species	deuterium eQq values (kHz)
HD−OCS	16(4)[39,a]
o-D_2−OCS	30(2)[39]
HD−CuF	41.(3)[b]
o-D_2−^{63}CuF	47.(7)[b]
$ReD_2(CO)(NO)(PMe_3)_2$	70.0(10), 65.3(10)[67]
$ReD_2(CO)(NO)(PCy_3)_2$	69.5(10), 66.7(10)[67]
$ReD_2(CO)(NO)(PPr^i_3)_2$	71.0(10), 68.8(10)[67]

[a]Numbers in parentheses give standard errors (1σ, 67% confidence level) in units of the least significant figure. [b]This work.

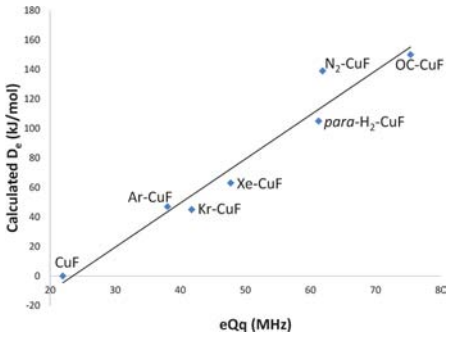

Figure 6. Graph of the calculated dissociation energies versus the eQq values from Table 2. The data is well fit by a linear relationship despite inconsistencies in methodology and basis set choice across the group.[42,58−61,64] The line is the least-squares fit of the data points to an assumed straight line.

Molecular orbital (MO), natural bond order (NBO), vibrational frequency, and energy calculations were used to compare properties of H_2 and CuF monomers to those of the complex. The σ donation theory mentioned above implies that there exists an appropriate empty orbital on the metal for electron donation from the σ orbital of H_2, and there is also a filled orbital on the metal that can easily overlap with that of H_2's antibonding orbital, σ^*.[16−18] A schematic of this overlap is given in Figure 5. Around the schematic are pictures of the calculated MOs from the individual monomers H_2 and CuF. The more interesting result is the orbitals in the complex. There is overlap of the bonding orbital of H_2 with an empty LUMO (largely s in character) on the Cu of the CuF, and there is π-type overlap between the filled orbital with the antibonding σ^* orbital of H_2. This backbonding should result in an elongating of the H−H bond distance. Future experiments will test whether the H−H bond in the complex is indeed longer than the H−H distance in H_2 itself.

Natural bond order (NBO) analysis of the complex along with the monomer substituents was carried out to determine whether there is any significant change in the charge on the atoms upon complexation. In the monomers, charges of +0.796|e| for Cu and −0.796|e| for F in CuF were calculated, as expected for a largely ionic bond. Zero, of course, was the value for the charges on each H in the H_2 monomer. Again, the interesting result was for H_2−CuF where, upon complexation, +0.033|e| for each H, +0.685|e| for Cu, and −0.752|e| for F was calculated. A charge decrease of over 0.1 on the copper, signifying a large amount of electron density being moved onto the copper upon complexation with hydrogen, is in accordance with the donation of electrons from H_2. H_2's charge, in turn, increased in value, signifying an overall loss of electron density on the hydrogen. Fluorine's charge was relatively unchanged but decreased in magnitude, becoming more positive representing a loss of electron density on the fluorine. This loss of electron density signifies more electron sharing between the fluorine and copper atoms. This is experimentally confirmed by the shrinking of the Cu−F bond length upon complexation, which will be discussed later in the section.

Lastly, vibrational frequency and energy analyses were carried out theoretically and compared to known dihydrogen complexes in the literature. These results are summarized in Table 4. Upon applying zero point energy corrections, the dissociation energy, D_e, was adjusted to the D_0 value of 60.2 kJ mol^{-1} showing that the complex is a viable, stable species instead of breaking down or weakening substantially in the ground vibrational state. Second, to help show that elongation of the H−H bond is possible, an analysis of the H−H harmonic stretching frequency (v = 1) was undertaken. If elongation is to occur, then the v = 1 value should decrease upon complexation. In order to identify which vibrational mode was v = 1, GaussView 5.0 again was utilized. In this mode, H_2 stretches with small or no movement of the CuF species. Upon inspection of the table, this value changes from 4407 cm^{-1} in

dx.doi.org/10.1021/ic301941k | Inorg. Chem. 2013, 52, 816−822

Table 4. Calculated Parameters of the H_2−CuF Complex and Literature Comparisons

parameter	value
D_e, kJ mol^{-1}	105.1[a]
D_0, kJ mol^{-1}	60.2[a]
complex ν(H−H) (v = 1), cm^{-1}	3348[a]
H_2−CuCl ν(H−H), cm^{-1}	3222[68]
Cu^+−H_2 (Theoretical) ν(H−H), cm^{-1}	3772[69]
Ag^+−H_2 ν(H−H), cm^{-1}	3750.56[70]
$Cr(CO)_5(H_2)$ ν(H−H), cm^{-1}	3030[71]
$Mo(CO)_5(H_2)$ ν(H−H), cm^{-1}	3080[72]
$W(CO)_3(PCy_3)_2(H_2)$ ν(H−H), cm^{-1}	2690[11]
free H_2 ν(H−H) (Theoretical), cm^{-1}	4407[a]
free H_2 ν(H−H) (Experimental), cm^{-1}	4160.2[73]

[a]This work.

the calculated free H_2 to 3348 cm^{-1} in the complex, a significant decrease in frequency. The value of 3348 cm^{-1} also seems reasonable considering it lies between the experimental value of 3222 cm^{-1} for H_2−CuCl (3222 cm^{-1})[68] and the theoretical value of Cu^+−H_2 (3772 cm^{-1})[69] and is in accordance with other known dihydrogen complexes in Table 4. The difference in the calculated H_2 stretching frequency from experiment is also reasonable considering only harmonic values were considered.

While we cannot, at this time, experimentally determine the H−H distance in the H_2−CuF complex, our data does allow us to determine the center-of-mass of H_2 to Cu (H_2−Cu) distance and the Cu−F distance in the complex. We calculate the values of these two parameters that best reproduce, in a least-squared sense, the measured values of $(B + C)/2$ for the six isotopologues given in Table 1. The resulting geometry is called an r_0 structure, and to do this we used the STRFIT program by Kisiel[74] available on the PROSPE Web site.[75] We have two choices when determining r_0(H_2−Cu) and r_0(Cu−F); we can assume that the H−H distance in the complex is the measured distance in H_2, 0.7505931 Å,[76] or we can use the APF-D calculated, elongated, r_0 value for this distance, 0.838 Å. The first choice gives an r_0(H_2−Cu) value of 1.5246(5) Å and an r_0(Cu−F) value of 1.7409(1) Å; the second choice gives 1.5198(5) Å and 1.7409(1) Å, respectively. The Cu−F distance in diatomic CuF is 1.7486 Å.[42] Thus, we have determined that the Cu−F distance contracts by 0.0077 Å upon complexation with H_2, in agreement with the molecular orbital picture of the bonding presented above. These results are summarized in Table 5.

We are in the process of extending the frequency limits of the spectrometer to 40 GHz. When completed, further investigations on the structure will be carried out and reported in more detail.

CONCLUSIONS

The authors have presented a chemical bonding investigation of the dihydrogen complex, H_2−CuF. The J = 1−0 transitions of six isotopologues of the complex have been observed, measured, and analyzed. Hydrogen complexation with the transition metal-containing molecule has been observed before, but this is the first gas phase rotational study of its kind. The rotational constant $(B + C)/2$, copper, fluorine, and deuterium hyperfine constants have been determined and reported. The large deviation of the measured copper and deuterium eQq values in the complex from the uncomplexed eQq values implies the beginning of a chemical bond between the metal and hydrogen species. Theoretical MO diagrams, NBO analyses, binding energies, and vibrational energies support these observations.

ASSOCIATED CONTENT

Supporting Information

The transition assignments and measurements for all H_2−CuF isotopologues have been provided.

This material is available free of charge via the Internet at http://pubs.acs.org/.

AUTHOR INFORMATION

Corresponding Author

*E-mail: ggrubbs@wesleyan.edu.

Notes

The authors declare no competing financial interest.

ACKNOWLEDGMENTS

The authors acknowledge the support of the NSF, Grant CHE-1011214. We thank Wesleyan University for computer time supported by the NSF under Grant CNS-0619508. The authors also thank Mike Frisch and George Petersson for their permission for us to use the Gaussian Developmental Program Suite along with the early use of the density functional APF-D method.

REFERENCES

(1) Schlapbach, L. *Mater. Res. Soc. Bull.* **2002**, *27*, 675.
(2) Schlapbach, L.; Züttel, A. *Nature* **2001**, *414*, 353.
(3) Thomas, K. M. *Catal. Today* **2007**, *120*, 389.
(4) Morris, R. E.; Wheatley, P. S. *Angew. Chem., Int. Ed.* **2008**, *47*, 4966.
(5) Dinca, M.; Long, J. R. *Angew. Chem., Int. Ed.* **2008**, *47*, 6766.
(6) Kondo, M.; Yoshitomi, T.; Seki, K.; Matsuzaka, H.; Kitagawa, S. *Angew. Chem., Int. Ed.* **1997**, *36*, 1725.
(7) Rosi, N. L.; Eckert, J.; Eddaoudi, M.; Vodak, D. T.; Kim, J.; O'Keeffe, M.; Yaghi, O. M. *Science* **2003**, *300*, 1127.
(8) Thomas, K. M. *Dalton Trans.* **2009**, 1487.
(9) Kuppler, R. J.; Timmons, D. J.; Fang, Q.-R.; Li, J.-R.; Makal, T. A.; Young, M. D.; Yuan, D.; Zhuang, W.; Zhou, H.-C. *Coord. Chem. Rev.* **2009**, *253*, 3042.

Table 5. Reported, Calculated, and Semi-Experimental[74,a] r_0 Structures

measurement	monomer	calculated[b]	semi-experimental	
Cu−F, Å	1.7486486(2)[42,c,d]	1.745	1.7409(1)	1.7409(1)
H−H, Å	0.7505931[76,d]	0.838	0.7505931[e]	0.838[e]
C.O.M. H_2−CuF, Å		1.523	1.5246(5)	1.5198(5)

[a]See text for details. [b]APF-D/aug-cc-pVQZ with Cu ECP10MDF vibrationally averaged structure. [c]Numbers in parentheses give standard errors (1σ, 67% confidence level) in units of the least significant figure. [d]Determined from reference values; error in value is error in measurement. [e]Parameter held to this value.

(10) Long, J. R.; Yaghi, O. M. *Chem. Soc. Rev.* **2009**, *38*, 1213.
(11) Kubas, G. J.; Ryan, R. R.; Swanson, B. I.; Vergamini, P. J.; Wasserman, H. J. *J. Am. Chem. Soc.* **1984**, *106*, 451.
(12) McGrady, G. S.; Guilera, G. *Chem. Soc. Rev.* **2003**, *32*, 383.
(13) Perutz, R. N.; Sabo-Etienne, S. *Angew. Chem., Int. Ed.* **2007**, *46*, 2578.
(14) Heinekey, D. M.; Lledós, A.; Lluch, J. M. *Chem. Soc. Rev.* **2004**, *33*, 175.
(15) Kubas, G. J. *Proc. Natl. Acad. Sci. U.S.A.* **2007**, *104*, 6901.
(16) Crabtree, R. H. *Angew. Chem., Int. Ed. Engl.* **1993**, *32*, 789.
(17) Kubas, G. J. *Acc. Chem. Res.* **1988**, *21*, 789.
(18) Devarajan, D.; Ess, D. H. *Inorg. Chem.* **2012**, *51*, 6367.
(19) Hebden, T. J.; Goldberg, K. I.; Heinekey, D. M.; Zhang, X.; Emge, T. J.; Goldman, A. S.; Krogh-Jespersen, K. *Inorg. Chem.* **2010**, *49*, 1733.
(20) Jean, Y.; Eisenstein, O.; Volatron, F.; Maouche, B.; Sefta, F. *J. Am. Chem. Soc.* **1986**, *108*, 6587.
(21) Bau, R.; Drabnis, M. H. *Inorg. Chim. Acta* **1997**, *259*, 27.
(22) Zilm, K. W.; Millar, J. M. *Adv. Magn. Opt. Reson.* **1990**, *15*, 163.
(23) Hamilton, D. G.; Crabtree, R. H. *J. Am. Chem. Soc.* **1988**, *110*, 4126.
(24) Desrosiers, P. J.; Cai, L.; Lin, Z.; Richards, R.; Halpern, J. *J. Am. Chem. Soc.* **1991**, *113*, 4173.
(25) Luther, T. A.; Heinekey, D. M. *Inorg. Chem.* **1998**, *37*, 127.
(26) Eckert, J.; Kubas, G. J. *J. Phys. Chem. A* **1993**, *97*, 2378.
(27) Zhao, D.; Yuan, D.; Zhou, H.-C. *Energy Environ. Sci.* **2008**, *1*, 222.
(28) Eddaoudi, M.; Eubank, J. F. In *Organic Nanostructures*; Atwood, J. L., Steed, J. W. Wiley-VCH: 2008; pp 251−274.
(29) Balle, T. J.; Campbell, E. J.; Keenan, M. R.; Flygare, W. H. *J. Chem. Phys.* **1979**, *71*, 2723.
(30) Balle, T. J.; Campbell, E. J.; Keenan, M. R.; Flygare, W. H. *J. Chem. Phys.* **1980**, *72*, 922.
(31) Pratt, D. W. *Annu. Rev. Phys. Chem.* **1998**, *49*, 481.
(32) Arunan, E.; Dev, S.; Mandal, P. K. *Appl. Spectrosc. Rev.* **2004**, 131.
(33) Walker, N. R. *Philos. Trans. R. Soc. A* **2007**, *365*, 2813.
(34) Steber, A. L.; Neil, J. L.; Zaleski, D. P.; Pate, B. H.; Lesarri, A.; Bird, R. G.; Vaquero-Vara, V.; Pratt, D. W. *Faraday Discuss. Chem. Soc.* **2011**, *150*, 227.
(35) Balle, T. J.; Flygare, W. H. *Rev. Sci. Instrum.* **1981**, *52*, 33.
(36) Walker, A. R. H.; Chen, W.; Novick, S. E.; Bean, B. D.; Marshall, M. D. *J. Chem. Phys.* **1995**, *102*, 7298.
(37) Frohman, D. J.; Grubbs, G. S., II; Novick, S. E. *J. Mol. Spectrosc.* **2011**, *270*, 40.
(38) Walker, K. A.; Gerry, M. C. L. *J. Mol. Spectrosc.* **1997**, *182*, 178.
(39) Yu, Z.; Higgins, K. J.; Klemperer, W.; McCarthy, M. C.; Thaddeus, P. *J. Chem. Phys.* **2005**, *123*, 221106.
(40) Yu, Z.; Higgins, K. J.; Klemperer, W.; McCarthy, M. C.; Thaddeus, P.; Liao, K.; Jäger, W. *J. Chem. Phys.* **2007**, *127*, 054305.
(41) Michaud, J. M.; Liao, K.; Jäger, W. *Mol. Phys.* **2008**, *106*, 23.
(42) Evans, C. J.; Gerry, M. C. L. *J. Chem. Phys.* **2000**, *112*, 9363.
(43) McClelland, G. M.; Saenger, K. L.; Valentini, J. J.; Herschbach, D. R. *J. Phys. Chem. A* **1979**, *83*, 947.
(44) Tarbutt, M. R.; Hudson, J. J.; Sauer, B. E.; Hinds, E. A.; Ryzhov, V. A.; Ryabov, V. L.; Ezhov, V. F. *J. Phys. B: At., Mol. Opt. Phys.* **2002**, *35*, 5013.
(45) Hensel, K. D.; Styger, C.; Jäger, W.; Merer, A. J.; Gerry, M. C. L. *J. Chem. Phys.* **1993**, *99*, 3320.
(46) Frisch, M. J.; et al. *Gaussian Development Version*, Revision H.11; Gaussian, Inc.: Wallingford, CT, 2010.
(47) Austin, A.; Petersson, G. A.; Frisch, M. J.; Dobek, F. J.; Scalmani, G.; Throssell, K. *J. Chem. Theor. Comput.* **2012**, *8*, 4989 DOI: 10.1021/ct300778e.
(48) Dunning, T. H. *J. Chem. Phys.* **1989**, *90*, 1007.
(49) Figgen, D.; Rauhut, G.; Dolg, M.; Stoll, H. *Chem. Phys.* **2005**, *311*, 227.
(50) Peterson, K. A.; Puzzarini, C. *Theor. Chem. Acc.* **2005**, *114*, 283.
(51) Stuttgart and Cologne Group. http://www.theochem.uni-stuttgart.de/pseudopotentials/clickpse.en.html.
(52) Dennington, R.; Keith, T. A.; Millam, J. M. *GaussView 5.0*; Gaussian, Inc.: Wallingford, CT, 2000−2008.
(53) Pickett, H. M. *J. Mol. Spectrosc.* **1991**, *148*, 371.
(54) Hoeft, J.; Lovas, F. J.; Tiemann, E.; Törring, T. *Z. Naturforsch.* **1970**, *25a*, 35.
(55) Townes, C. H.; Dailey, B. P. *J. Chem. Phys.* **1949**, *17*, 782.
(56) Gordy, W.; Cook, R. L. *Microwave Molecular Spectra; Techniques of Chemistry*; Wiley: New York, 1984; Vol. *XVIII*.
(57) Townes, C. H.; Schawlow, A. L. *Microwave Spectroscopy*; Dover Publications, Inc.: New York, 1975.
(58) Michaud, J. M.; Cooke, S. A.; Gerry, M. C. L. *Inorg. Chem.* **2004**, *43*, 3871.
(59) Michaud, J. M.; Gerry, M. C. L. *J. Am. Chem. Soc.* **2006**, *128*, 7613.
(60) Francis, S. G.; Matthews, S. L.; Poleshchuk, O. K.; Walker, N. R.; Legon, A. C. *Angew. Chem., Int. Ed.* **2006**, *45*, 6341.
(61) Walker, N. R.; Gerry, M. C. L. *Inorg. Chem.* **2001**, *40*, 6158.
(62) Lin, W.; Novick, S. E. *J. Mol. Spectrosc.* **2007**, *243*, 32.
(63) Kang, L.; Novick, S. E. *J. Mol. Spectrosc.* **2012**, *276−277*, 10.
(64) Bera, J. K.; Samuelson, A. G.; Chandresekhar, J. *Organometallics* **1998**, *17*, 4136.
(65) Novick, S. E. *J. Mol. Spectrosc.* **2011**, *267*, 13.
(66) Leopold, K. R.; Fraser, G. T.; Novick, S. E.; Klemperer, W. *Chem. Rev.* **1994**, *94*, 1807.
(67) Nietlispach, D.; Bakhmatov, V. I.; Berke, H. *J. Am. Chem. Soc.* **1993**, *115*, 9191.
(68) Plitt, H. S.; Bär, M. R.; Ahlrichs, R.; Schnöckel, H. *Angew. Chem., Int. Ed. Engl.* **1991**, *30*, 832.
(69) Kemper, P. R.; Weis, P.; Bowers, M. T.; Maître, P. *J. Am. Chem. Soc.* **1998**, *120*, 13494.
(70) Dryza, V.; Bieske, E. J. *J. Phys. Chem. Lett.* **2011**, *2*, 719.
(71) Upmacis, R. K.; Gadd, G. E.; Poliakoff, M.; Simpson, M. B.; Turner, J. J.; Whyman, R.; Simpson, A. F. *J. Chem. Soc., Chem. Commun.* **1985**, *14*, 27.
(72) Heinekey, D. M.; Oldham, W. J. *Chem. Rev.* **1993**, *93*, 913.
(73) Teal, G.; MacWood, G. E. *J. Chem. Phys.* **1935**, *3*, 760.
(74) Kisiel, Z. *J. Mol. Spectrosc.* **2003**, *218*, 58.
(75) Kisiel, Z. http://info.ifpan.edu.pl/kisiel/prospe.htm.
(76) Huber, K. P.; Herzberg, G. *Molecular Spectra and Molecular Structure IV. Constants of Diatomic Molecules*; Van Nostrand Reinhold Company/Litton Educational Publishing: New York, 1979.